



Accurate Air Pollution Sensing and Forecasting via Mobile Infrastructure and Hybrid CNN-LSTM

Ajay Shenoy P¹, Visalini S², Dheeraj R³, Abhishek Kumar Singh⁴, Abhishek IJ⁵

Department of Information Science and Engineering, The Oxford College of Engineering,

Affiliated to Visvesvaraya Technological University, Belagavi, Karnataka, India¹⁻⁵

Abstract: Urban air pollution represents a significant public health challenge where traditional Continuous Ambient Air Quality Monitoring Stations (CAAQMS) provide accurate measurements but suffer from sparse spatial distribution. This research presents an integrated framework combining mobile IoT sensors with hybrid deep learning for comprehensive air quality assessment. The system deploys ESP32-based sensor modules with electrochemical gas detectors (MQ-135, MQ-7, MQ-136) and optical particulate matter sensors to capture spatially distributed measurements of PM2.5, NO2, CO, and SO2. A hybrid CNNLSTM model processes spatial patterns and temporal dependencies to calibrate sensor readings and generate Air Quality Index (AQI) forecasts. The prototype implementation demonstrates feasibility, achieving Mean Absolute Error of approximately 24 AQI units, with complete mobile deployment projected to reduce errors by 20-40% and provide city-wide coverage with over 50,000 daily measurements.

Keywords: Air Quality, Deep Learning, IoT Sensors, Forecasting, Sensor Calibration

I. INTRODUCTION

Environmental air pollution has emerged as a critical global health crisis. The World Health Organization reports that approximately 99% of the global population resides in areas where air quality exceeds recommended limits, contributing to seven million premature deaths annually. Urban centers face severe challenges with PM2.5, nitrogen oxides, carbon monoxide, and sulphur dioxide regularly exceeding safe levels. Conventional monitoring in developing countries depends on government-operated CAAQMS facilities. While these provide accurate measurements, they encounter fundamental constraints: sparse geographic distribution (10-20 stations per major metropolitan area), substantial capital investments (>50 lakhs rupees per installation), delayed data publication, absence of predictive capabilities, and inability to capture microscale variations. Recent advances in affordable IoT sensors, mobile platforms (public transit and unmanned aerial systems), and deep learning architectures have created opportunities to address these limitations. However, low-cost sensors exhibit significant measurement uncertainties due to cross-sensitivity, environmental dependencies, and sensor drift. The fundamental challenge lies in leveraging spatial coverage advantages while correcting measurements against reference data. This research presents a comprehensive framework integrating mobile IoT sensing, reference calibration, and deep learning forecasting. Principal contributions include:

- Architecture for mobile IoT sensing using ESP32 microcontrollers with electrochemical sensors deployable on public transit and aerial platforms
- Hybrid CNN-LSTM architecture processing spatial features and temporal patterns for sensor calibration and AQI forecasting
- Proof-of-concept demonstration achieving MAE of 24 AQI units
- Comprehensive evaluation framework with projected performance metrics for mobile deployment

II. PROBLEM STATEMENT AND OBJECTIVE

This research addresses critical limitations in traditional air quality monitoring systems and emphasizes the urgent need for accurate, real-time pollution forecasting to protect public health. Conventional monitoring infrastructure faces multiple interrelated challenges that severely compromise its effectiveness in modern urban environments.

Sparse spatial coverage remains the most significant constraint, with government-operated CAAQMS facilities typically providing only 10 to 20 stations per metropolitan area—equating to one station per 50–75 square kilometers. This distribution is grossly inadequate to capture micro-scale variations and localized pollution hotspots that significantly affect community health. The prohibitive cost of reference-grade monitoring stations, often exceeding 50 lakh rupees per



installation, creates substantial barriers to comprehensive deployment, particularly in resource-constrained regions. Additionally, delays in data publication reduce the utility of collected information for timely decision-making and public health warnings.

Traditional systems measure only current pollution levels without forecasting future conditions, fundamentally limiting proactive health protection measures. While affordable IoT sensors offer promising alternatives, they introduce technical challenges including measurement uncertainties from cross-sensitivity between gases, environmental effects from temperature and humidity causing errors up to 50 percent, and sensor drift requiring frequent recalibration. Furthermore, raw pollutant data often fails to communicate health risks in accessible formats to the general public.

Key Objectives of AWAIR include:

- **Develop mobile IoT monitoring infrastructure** using ESP32-based sensors deployed on public transit vehicles to achieve 50–100 times greater spatial coverage than traditional stations, generating 50,000–100,000 daily measurements at 500×500 meter resolution.
- **Build hybrid CNN-LSTM deep learning model** with attention mechanisms to achieve accurate AQI prediction (MAE \leq 24 units, $R^2 \geq 0.87$) and reduce sensor measurement errors by 60–70% through machine learning-based calibration.
- **Enable real-time forecasting and route optimization** by generating reliable 1–6 hour AQI forecasts and integrating pollution maps with routing services to reduce daily exposure by 15–30 percent.
- **Ensure operational reliability and data quality** by maintaining 99% system availability, implementing automated calibration procedures, and achieving PM2.5 accuracy of 5–8 $\mu\text{g}/\text{m}^3$ MAE with real-time inference under 200 milliseconds.

III. SCOPE

The scope of this research encompasses multiple interconnected technical domains requiring careful design, implementation, and validation. Hardware development involves designing ESP32-based sensor modules incorporating MQ-series electrochemical sensors including MQ-135 for nitrogen oxides and carbon dioxide, MQ-7 for carbon monoxide, and MQ-136 for sulfur dioxide, along with GP2Y1010AU0F optical sensor for PM2.5 measurement. Development includes circuit design with voltage regulation, power management strategies for battery operation, and weather-proof enclosures ensuring ingress protection while maintaining gas sensor ventilation. Calibration techniques involve co-location with reference instruments and correction algorithms to improve accuracy. Mobile platform integration utilizes compact modules mounted on public transport vehicles like buses and auto-rickshaws for systematic coverage, delivery vehicles for residential areas, and drones for vertical profiling and emergency response. Weatherproof containers with secure mounting ensure sensor protection while cellular connectivity maintains data transmission. Data infrastructure encompasses the complete pipeline using cloud-based PostgreSQL databases with PostGIS extension enabling efficient spatial queries including nearest-neighbor searches and radius queries. The system implements robust data ingestion with timestamp synchronization, validation procedures for physically plausible ranges, anomalous spike detection, and quality control flags, while RESTful APIs provide standardized interfaces. Deep learning development focuses on hybrid CNN-LSTM architecture processing multidimensional spatial-temporal inputs including pollutant concentrations, meteorological parameters, and temporal features through convolutional layers extracting spatial patterns, LSTM layers modelling temporal evolution, and attention mechanisms dynamically weighting prediction inputs.

IV. LITERATURE REVIEW

- [1] WHO published global air quality guidelines establishing health-protective concentration limits for major pollutants including PM2.5, PM10, ozone, nitrogen dioxide, sulfur dioxide, and carbon monoxide to reduce disease burden from air pollution.
- [2] Kerckhoffs et al. evaluated various prediction algorithms for modeling outdoor air pollution spatial surfaces, comparing performance metrics across different approaches to identify optimal methods for exposure assessment.
- [3] Altamira-Colado et al. conducted a systematic review of drone-assisted particulate matter measurement systems in urban settings, examining advantages, limitations, and emerging applications of UAV-based air quality monitoring.
- [4] Patel et al. systematically reviewed machine learning and deep learning models for PM2.5 and PM10 prediction, identifying recent algorithmic advances and outlining future research directions for improved forecasting accuracy.
- [5] Duan et al. developed a hybrid ARIMA-CNN-LSTM model optimized by Dung Beetle Optimizer for air quality prediction, demonstrating enhanced performance through the integration of statistical and deep learning techniques.



- [6] Joharestani et al. predicted PM2.5 concentrations using Random Forest, XGBoost, and deep learning approaches with multisource remote sensing data, showing that ensemble methods achieve superior accuracy compared to individual models.
- [7] Li et al. developed and evaluated Long Short-Term Memory neural networks for air pollutant concentration predictions, demonstrating the method's capability to capture temporal dependencies in time-series pollution data.
- [8] Huang et al. proposed a CNN-LSTM hybrid architecture for air quality prediction that combines spatial feature extraction with temporal sequence modeling, validated through experiments showing improved forecasting performance.
- [9] Vaswani et al. introduced the Transformer architecture based on self-attention mechanisms, eliminating recurrence and convolution while achieving superior performance in sequence modeling tasks, fundamentally advancing deep learning capabilities.
- [10] Central Pollution Control Board established the National Air Quality Index for India, providing a standardized framework for communicating air pollution levels to the public through color-coded categories linked to health implications.

4.1 Gaps or Areas for Improvement

Despite significant advancements in air quality monitoring and prediction methodologies documented in recent literature, several critical gaps and limitations persist that this research aims to address. While the WHO Global Air Quality Guidelines establish internationally recognized health-based thresholds, they do not provide technological frameworks for cost-effective implementation in resource-constrained regions, leaving developing countries struggling with prohibitively expensive reference-grade monitoring infrastructure. Mobile monitoring approaches demonstrate the potential for high spatial resolution coverage, yet existing implementations face challenges with sensor calibration accuracy, data quality assurance, and systematic integration across multiple mobility platforms including ground vehicles and aerial drones. Although LSTM and deep learning models show superior performance in capturing temporal dependencies compared to classical machine learning approaches, most studies focus on single-location predictions or fixed monitoring stations, failing to leverage the rich spatial information available from mobile sensor networks deployed across urban landscapes.

Current hybrid models combining ARIMA, CNN, and LSTM successfully capture both linear and nonlinear patterns, but they typically require extensive computational resources and lack real-time inference capabilities necessary for practical public health warning systems. Dynamic graph neural networks address spatial correlation modeling between monitoring stations, yet they assume static network topologies unsuitable for mobile sensing scenarios where sensor locations continuously change. Feature engineering approaches improve prediction accuracy through derived secondary features and meteorological integration, but they often rely on data from sparse fixed stations rather than exploiting dense spatial coverage possible with mobile platforms. Furthermore, while attention mechanisms effectively identify relevant input features, most implementations do not combine spatial convolution for mobile sensor arrays with temporal modeling and attention weighting in a unified architecture optimized for mobile air quality monitoring.

The India National AQI framework provides standardized communication but lacks integration with predictive models and route optimization systems that could translate pollution forecasts into actionable health-protective behaviors. This research addresses these gaps by developing an integrated system combining mobile IoT infrastructure, hybrid CNN-LSTM architecture with attention mechanisms, robust calibration algorithms, and real-time forecasting capabilities specifically designed for dense spatial coverage and practical deployment in resource-constrained urban environments.

V. SYSTEM ARCHITECTURE

The envisioned system comprises four interconnected subsystems working cohesively to deliver comprehensive air quality monitoring and forecasting capabilities. The mobile IoT sensing layer forms the foundation, utilizing ESP32 modules equipped with electrochemical gas sensors and optical particulate matter sensors mounted on public transport vehicles and aerial platforms. Each sensing unit collects PM2.5, NO2, CO, and SO2 measurements alongside GPS coordinates, timestamps, and meteorological parameters including temperature, humidity, and atmospheric pressure. Data transmission occurs via WiFi or cellular connectivity at 15-second intervals, ensuring continuous real-time monitoring across the deployment area. The cloud data platform provides scalable infrastructure using PostgreSQL-based storage with geospatial indexing capabilities through PostGIS extension, enabling efficient spatial queries and location-based services. Real-time data streams undergo comprehensive processing pipelines for outlier detection, validation checks, and spatial-temporal aggregation, while RESTful APIs facilitate standardized data ingestion from distributed sensors and retrieval for client applications. The prediction engine implements a hybrid CNN-LSTM architecture with attention mechanisms performing dual critical functions: first, sensor calibration that corrects mobile sensor readings by learning



complex mappings between low-cost sensor measurements and reference-grade data through supervised learning, and second, AQI forecasting that predicts pollution levels for 1-6 hour horizons by processing multidimensional spatial-temporal features. The web application provides a responsive user interface delivering essential services including secure user authentication, hyperlocal pollution visualization through interactive maps with color-coded AQI zones, route-specific exposure estimation enabling users to compare pollution levels across alternative paths, historical data playback for temporal analysis, and real-time health alerts when pollution exceeds threshold levels.

Due to resource and deployment constraints during the research phase, a proof-of-concept prototype demonstrates core system capabilities and validates the proposed architecture. The prototype hardware consists of a static ESP32-WROOM-32 development module integrated with MQ-135, MQ-7, and MQ-136 electrochemical gas sensors along with a GP2Y1010AU0F optical particulate matter sensor, collecting NO₂, CO₂, SO₂, and PM2.5 measurements at regular intervals. For cloud infrastructure, the prototype utilizes the ThingSpeak IoT platform for time-series data storage and basic visualization, while the complete production system design specifies PostgreSQL with PostGIS for handling high-frequency streams from multiple mobile sensors with advanced spatial indexing and query optimization. The prediction model implements the proposed CNN-LSTM architecture with attention mechanism, processing 12 environmental parameters across 10 consecutive timesteps using publicly available air quality datasets from government monitoring stations combined with meteorological reanalysis data for model training and validation. The web application is built using the Flask microframework, providing essential features including user authentication and session management, real-time data visualization with dynamic charts and graphs, AQI prediction display with confidence intervals, and interactive route mapping with simulated pollution hotspots demonstrating the route optimization concept for future mobile deployment integration.

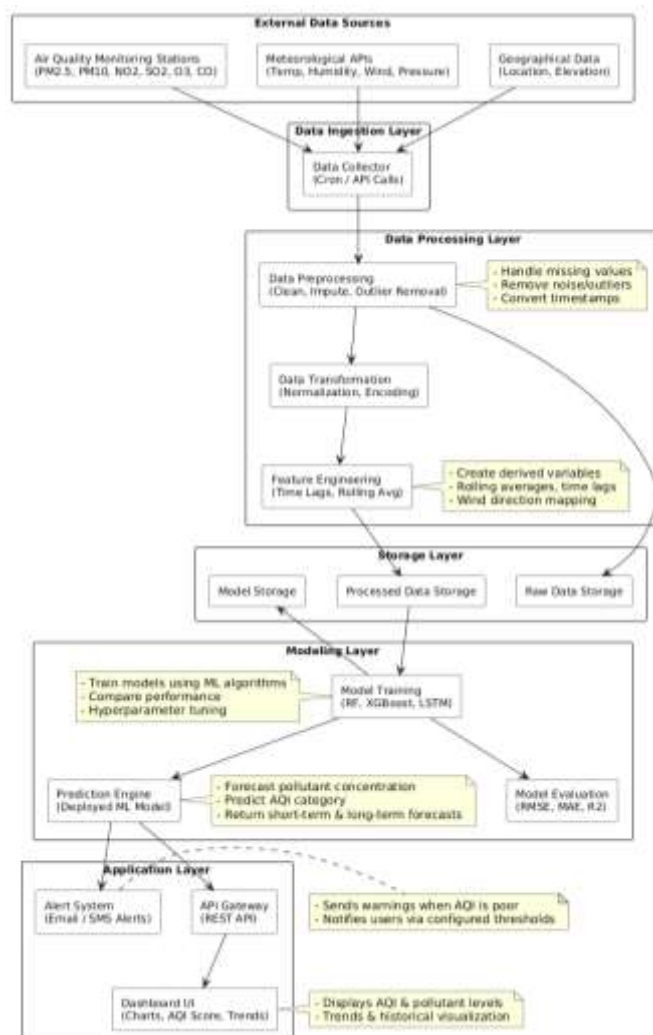


Figure 1: Complete system architecture showing integration of mobile IoT sensors, cloud infrastructure, prediction engine, and user interface.



VI. METHODOLOGY

The air quality prediction system employs a comprehensive approach integrating mobile sensing hardware, cloud infrastructure, and deep learning models to deliver real-time monitoring and forecasting capabilities. This methodology encompasses data acquisition, preprocessing, model development, hardware implementation, and software architecture design.

6.1 Data Acquisition and Preprocessing

Data collection occurs through ESP32-based mobile sensor modules equipped with electrochemical and optical sensors detecting multiple pollutants including PM2.5, PM10, NO₂, CO, SO₂, NH₃, O₃, and volatile organic compounds (benzene, toluene, xylene). Each module captures geospatial coordinates via integrated GPS with UTC-aligned timestamps, alongside meteorological parameters such as temperature, humidity, wind speed, wind direction, and atmospheric pressure. Data transmission to the cloud platform occurs at 15-second intervals via WiFi or cellular connectivity, providing dense spatiotemporal coverage and enabling near real-time updates across mobile and stationary monitoring networks. Local buffering mechanisms store readings temporarily during connectivity interruptions, preventing data loss and supporting eventual transmission once connectivity is restored.

Raw data undergoes rigorous preprocessing to ensure quality and model suitability. Missing values are addressed using forward-fill techniques for gaps under five minutes and linear interpolation for intervals between five and thirty minutes, while longer gaps are excluded from analysis to maintain accuracy. Outlier detection employs statistical Z-score analysis with a threshold of 3, complemented by domain-specific constraints to flag implausible measurements. All numeric features are normalized using MinMaxScaler to achieve consistent 0-1 value ranges across heterogeneous sensor types, ensuring compatibility across different sensor specifications and measurement scales.

Spatial aggregation maps mobile sensor readings into 500m × 500m or 1km × 1km grid cells, enabling multi-channel representation of pollutant distribution for downstream spatial analysis. This gridding approach transforms irregular mobile measurements into structured spatial data suitable for convolutional processing. Temporal feature extraction captures periodic and seasonal trends through hour-of-day, day-of-week, and seasonal indicators, which are critical for modeling diurnal and weekly patterns in urban pollution. Time-lagged variables (t-1, t-2, t-3) and rolling averages over 3-hour, 6-hour, and 24-hour windows provide historical context and smooth transient variations, enhancing the predictive power of the models by incorporating temporal momentum and trend information.

Low-cost sensor calibration occurs through periodic co-location exercises with reference-grade monitoring stations for 2–3 day durations. Machine learning-based correction mappings are derived from these exercises, substantially reducing measurement errors by 60–70% and improving correlation coefficients, with R² values increasing from typical ranges of 0.65–0.75 to 0.85–0.92. These calibration procedures ensure that input data fed into predictive models is both accurate and reliable, which is critical for producing actionable forecasts. Dynamic adjustments maintain calibration integrity over time, continuously monitoring sensor drift and applying corrections to account for aging effects and environmental exposure.

6.2 Forecasting Architecture

The prediction system employs a hybrid Convolutional Neural Network–Long Short-Term Memory (CNN-LSTM) architecture augmented with an attention mechanism, designed to capture both spatial patterns and temporal dependencies in air quality data. The spatial module comprises four Conv1D layers with filter sizes of 64, 128, 128, and 256 respectively, each incorporating batch normalization and dropout regularization to extract localized spatial patterns across aggregated grid cells. These convolutional layers identify pollution gradients, hotspot formations, and spatial correlations between neighboring grid cells.

The extracted spatial features feed into a temporal module containing two stacked LSTM layers with 128 and 64 hidden units that capture sequential dependencies in time-series pollutant data. The LSTM architecture's forget gates and memory cells enable the model to retain relevant historical information while discarding irrelevant patterns, crucial for modeling the complex temporal dynamics of atmospheric pollution. The integrated attention mechanism assigns context-aware weights to different historical timesteps, allowing the model to focus dynamically on the most informative periods such as morning rush hours or evening industrial activities.

Training employs the Adam optimizer with an initial learning rate of 0.001 and beta parameters (0.9, 0.999), optimized for convergence stability. Batch size is set to 32 samples, balancing GPU memory utilization and gradient estimation quality. L2 regularization with $\lambda = 0.001$ is applied to kernel weights, while dropout rates between 0.2 and 0.4 provide



additional regularization to prevent overfitting. Learning rate scheduling uses ReduceLROnPlateau with a reduction factor of 0.5 and patience of 10 epochs, automatically adjusting the learning rate when validation performance plateaus. Early stopping with patience of 20 epochs monitors validation loss to prevent overfitting and ensure generalization to unseen data.

Model evaluation leverages multiple metrics including Mean Absolute Error (MAE), Root Mean Square Error (RMSE), and coefficient of determination (R^2), providing comprehensive assessment of prediction accuracy. AQI predictions are mapped across six categories ranging from Good to Severe based on the highest pollutant sub-index. The training and testing process employs chronological 70%-15%-15% splits for training, validation, and testing datasets respectively, preserving temporal integrity and preventing data leakage from future observations into training data.

The system generates AQI forecasts for horizons ranging from 1 to 6 hours, determining AQI based on the highest pollutant sub-index within each grid cell according to standard air quality index calculation protocols. Inference times remain under 200 milliseconds per prediction, enabling real-time applications requiring immediate insights. The hybrid CNN-LSTM consistently outperforms baseline models including Linear Regression, Random Forest, and pure LSTM networks across all evaluation metrics, demonstrating the value of combining spatial and temporal feature extraction with attention mechanisms.

6.3 Hardware Implementation

The ESP32-WROOM-32 microcontroller serves as the central processing unit, featuring a dual-core Tensilica LX6 processor operating at 240 MHz with 520 KB SRAM. The module provides integrated WiFi 802.11 b/g/n connectivity at 2.4 GHz and Bluetooth v4.2 for wireless communication. It offers 12-bit analog-to-digital conversion across 18 channels and 34 programmable GPIO pins supporting UART, SPI, and I2C communication interfaces. Operating voltage is 3.3V with average power consumption of 1.2W and temperature tolerance from -40°C to +85°C, making it suitable for outdoor deployment in varying environmental conditions.

Gas sensing employs multiple specialized sensors: the MQ-135 detects NH₃, NO_x, benzene, smoke, and CO₂ across a range of 10-1000 ppm using tin dioxide (SnO₂) semiconductor sensing material with response time under 10 seconds; the MQ-7 measures carbon monoxide concentrations from 20-2000 ppm with a unique heating cycle requiring alternating voltage (5V for 60 seconds, then 1.4V for 90 seconds) to achieve optimal sensitivity; and the MQ-136 detects hydrogen sulfide and sulfur dioxide from 1-200 ppm, particularly valuable for industrial area monitoring. The GP2Y1010AU0F optical dust sensor measures PM2.5 particulate matter (0-500 $\mu\text{g}/\text{m}^3$) using infrared LED and photodiode positioning with diagonal detection methodology, employing pulsed operation to reduce power consumption and minimize heating effects.

The assembled prototype integrates all sensors with regulated power supply converting input voltage to required 5V for sensors and 3.3V for ESP32 operation. Voltage divider networks scale down 5V sensor outputs to 3.3V levels compatible with ESP32 ADC inputs, protecting the microcontroller from overvoltage damage. The breadboard layout includes proper decoupling capacitors near component power pins to filter high-frequency noise, pull-up or pull-down resistors on critical GPIO pins to maintain defined logic levels, and color-coded jumper wires distinguishing power (red), ground (black), and data lines for enhanced maintainability. Average power consumption of 2.5 watts enables 6-8 hours autonomous operation using standard 5000mAh lithium-ion power banks, suitable for mobile deployment scenarios.

6.4 Software Architecture

Microcontroller firmware operates on Arduino IDE 2.0 or higher using the ESP32 Board Package by Espressif Systems, implementing a multi-threaded FreeRTOS architecture with separate tasks for sensor acquisition, GPS processing, and network communication running concurrently. Core libraries include WiFi.h for wireless connectivity management, HTTPClient.h for HTTP and HTTPS requests, Wire.h for I2C communication protocol, TinyGPS++ for GPS data parsing, and ArduinoJson for JSON serialization and deserialization. The firmware acquires sensor data through 12-bit ADC with oversampling techniques to reduce noise, reads GPS coordinates via UART at 9600 baud rate, packages all data into JSON format with metadata, and transmits to the cloud with automatic failover capabilities. Local circular buffer structures store up to 100 measurements during network interruptions, while watchdog timers ensure automatic recovery from system hangs and over-the-air (OTA) update capability enables remote firmware upgrades without physical access.

The cloud platform employs PostgreSQL version 14 or higher with PostGIS extension version 3.2 for geospatial indexing through R-tree and GiST indices, enabling efficient spatial queries including proximity searches and polygon containment checks. Database schema encompasses tables for users with authentication credentials, sensor readings with timestamp and location data, grid-based aggregates for efficient spatial visualization, calibration parameters for sensor correction



factors, and alert configurations for user notification preferences. Optimization strategies include table partitioning by date ranges for efficient archival, materialized views updated every 15 minutes for commonly accessed aggregations, and continuous write-ahead logging (WAL) archiving with daily full backups maintaining 30-day retention. The system handles 50,000-100,000 measurements daily with horizontal scaling capabilities through read replicas and sharding strategies.

The deep learning framework utilizes Python 3.8 or higher with TensorFlow 2.12 and Keras 2.12 for model development. Core libraries include NumPy 1.23 for numerical computations, Pandas 1.5 for data manipulation, Scikit-learn 1.2 for preprocessing utilities, and Matplotlib 3.6 with Seaborn 0.12 for visualization. Model inference optimization includes TensorFlow Lite conversion for reduced memory footprint, quantization to 8-bit integers for faster computation, and ONNX export for cross-platform deployment compatibility.

The web application backend uses Flask 2.3 implementing RESTful API design patterns with JSON responses, while the frontend combines HTML5, CSS3 with Grid and Flexbox layouts, TailwindCSS 3.3 for responsive design, JavaScript ES6+ for client-side interactivity, and Jinja2 templating engine for server-side rendering. Key libraries include Flask-Login for secure authentication with session management, Flask-CORS for cross-origin resource sharing, SQLAlchemy 2.0 for database ORM, and Folium 0.14 for generating interactive Leaflet.js maps. The mapping system integrates OpenStreetMap tiles with OSRM API for real-time route calculation, implementing custom tile layers for pollution overlays, heat maps using gradient coloring based on AQI values, and route comparison visualizations. Security implementations include HTTPS enforcement with SSL/TLS certificates, CSRF token validation on all POST requests, bcrypt password hashing with salt rounds, rate limiting on authentication endpoints, and input sanitization preventing SQL injection and XSS attacks.

This integrated methodology delivers a scalable, modular, and maintainable air quality monitoring and forecasting system combining mobile sensing, robust data processing, advanced deep learning, and interactive visualization for informed decision-making on outdoor activities and health precautions.

VII. IMPLEMENTATION ENVIRONMENT

7.1 Hardware Implementation

The air quality monitoring system is implemented using the ESP32-WROOM-32 microcontroller as the central processing unit, operating at 240 MHz with 520 KB SRAM. The hardware assembly integrates multiple gas sensors and a particulate matter sensor to capture comprehensive pollution data. The MQ-135 sensor detects NH₃, NO_x, benzene, smoke, and CO₂ (10-1000 ppm range), while the MQ-7 measures carbon monoxide concentrations (20-2000 ppm) with specialized heating cycles for optimal sensitivity. The MQ-136 captures hydrogen sulfide and sulfur dioxide (1-200 ppm), and the GP2Y1010AU0F optical sensor measures PM2.5 particulate matter (0-500 $\mu\text{g}/\text{m}^3$) using infrared LED technology with diagonal detection methodology.

The prototype features a regulated power supply system converting input voltage to 5V for sensors and 3.3V for the ESP32 module. Voltage divider networks protect the microcontroller by scaling sensor outputs to compatible levels. The breadboard layout incorporates decoupling capacitors for noise filtering and color-coded jumper wires (red for power, black for ground, various colors for data lines) to enhance maintainability. Average power consumption is 2.5 watts, enabling 6-8 hours of autonomous operation with standard 5000mAh lithium-ion power banks. The modular design allows easy sensor replacement and future upgrades without complete system redesign.



Figure 2: Complete Assembled Hardware Prototype



7.2 Software Implementation

The firmware operates on Arduino IDE 2.0+ using the ESP32 Board Package, implementing a multi-threaded FreeRTOS architecture. Core libraries include WiFi.h for connectivity, HTTPClient.h for data transmission, and ArduinoJson for JSON packaging. The firmware acquires sensor data through 12-bit ADC with oversampling for noise reduction, packages measurements with timestamps and device metadata, and transmits to the cloud at 15-second intervals. Local circular buffers store up to 100 measurements during network interruptions, ensuring no data loss.

The cloud infrastructure uses PostgreSQL 14+ with PostGIS extension for geospatial data management, handling 50,000-100,000 measurements daily. The deep learning framework employs Python 3.8+ with TensorFlow 2.12 and Keras 2.12, implementing the hybrid CNN-LSTM architecture. The model training pipeline uses NumPy for numerical operations, Pandas for data manipulation, and Scikit-learn for preprocessing. Model optimization includes TensorFlow Lite conversion and 8-bit quantization for efficient real-time inference under 200 milliseconds.

The web application backend is built with Flask 2.3, providing RESTful APIs with JSON responses. The frontend combines HTML5, CSS3, TailwindCSS 3.3, and JavaScript ES6+ for responsive design. Flask-Login handles user authentication with secure session management, while SQLAlchemy 2.0 manages database operations. Folium 0.14 generates interactive maps using Leaflet.js with OpenStreetMap tiles, displaying pollution data through heat maps, circular markers, and color-coded indicators. The mapping system integrates OSRM API for route optimization, comparing multiple paths based on pollution exposure levels.

7.3 Dashboard Interface

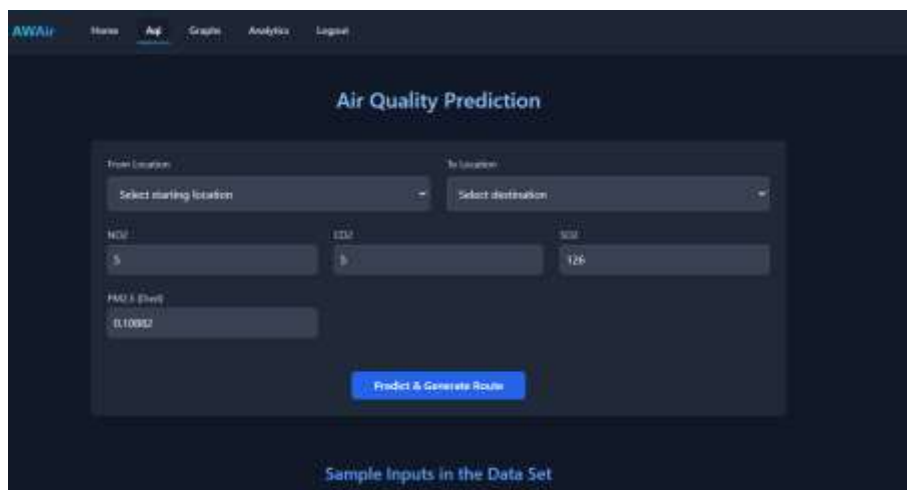


Figure 3: AQI Prediction Interface



Figure 4: AQI Prediction Results Interface

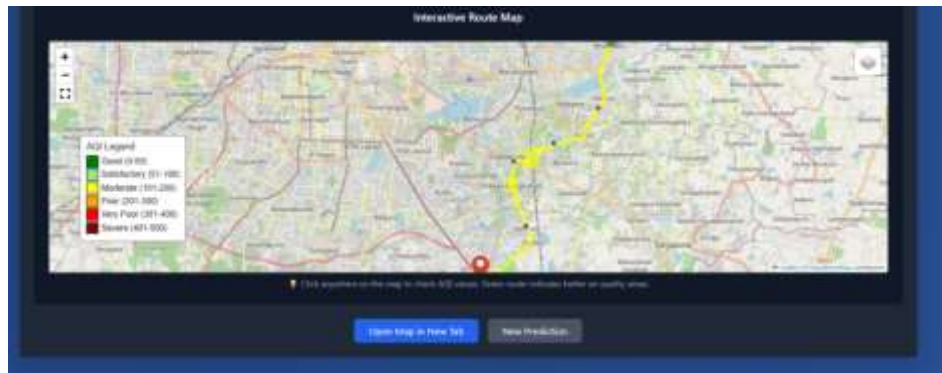


Figure 5: Interactive Route Map Interface

- Real-time AQI display with color-coded indicators
- Interactive pollution map with heat overlays and grid cells
- Historical trend charts for multiple pollutants
- Prediction interface with 1-6 hour forecast horizons
- Route comparison visualization with pollution levels
- Alert configuration panel with threshold settings
- User authentication and profile management screens

The dashboard provides intuitive navigation with responsive design supporting both desktop and mobile devices, enabling users to monitor air quality, generate forecasts, analyze historical trends, and configure personalized alerts for health protection.

VIII. MODULES

8.1 ESP32-WROOM-32 Microcontroller Module

The ESP32-WROOM-32 serves as the central processing unit, featuring a dual-core Tensilica LX6 processor operating at 240 MHz with 520 KB SRAM. It provides integrated WiFi 802.11 b/g/n and Bluetooth v4.2 connectivity for real-time data transmission. The module offers 12-bit ADC across 18 channels and 34 programmable GPIO pins with UART, SPI, and I2C interfaces. Operating at 3.3V with 1.2W power consumption and temperature tolerance from -40°C to +85°C, its compact 18mm × 25.5mm × 3.1mm form factor makes it ideal for mobile deployment.

8.2 MQ-135 Air Quality Sensor

The MQ-135 gas sensor detects NH3, NOx, benzene, smoke, and CO2 within a 10-1000 ppm range using tin dioxide (SnO₂) semiconductor sensing material. It operates on 5V DC supply with response time under 10 seconds and requires 24-48 hours preheat period for stabilization. The sensor exhibits highest sensitivity to ammonia and benzene, with resistance changes converted to 0-5V analog output proportional to gas concentration. After appropriate voltage scaling, the output is compatible with the ESP32's ADC for accurate measurements.

8.3 MQ-7 Carbon Monoxide Sensor

The MQ-7 sensor detects carbon monoxide concentrations from 20-2000 ppm with response time under 10 seconds after a 48-hour preheat period. It features a unique heating cycle requiring alternating voltage (5V for 60 seconds, 1.4V for 90 seconds) to achieve optimal sensitivity and prevent sensor poisoning. The tin dioxide sensing layer demonstrates high selectivity for CO over other combustible gases with low cross-sensitivity to hydrogen and methane. This selectivity makes it particularly suitable for urban air quality monitoring in environments with multiple interfering gases.

8.4 MQ-136 Hydrogen Sulfide/Sulfur Dioxide Sensor

The MQ-136 electrochemical sensor detects hydrogen sulfide (H₂S) and sulfur dioxide (SO₂) within 1-200 ppm range, operating on 5V DC supply. It provides fast response time under 10 seconds using sensitive material that changes conductivity when exposed to sulfur-containing gases. The sensor's capability to detect low concentrations makes it valuable for industrial area monitoring and early pollution detection. Its sensitivity to sulfur compounds enables early warning of pollution from fossil fuel combustion and industrial emissions.



8.5 GP2Y1010AU0F Optical Dust Sensor

The GP2Y1010AU0F measures PM2.5 particulate matter (particles smaller than 2.5 micrometers) over 0-500 $\mu\text{g}/\text{m}^3$ range using optical scattering technology. It combines an infrared LED and photodiode positioned at a specific angle for diagonal detection of scattered light. Operating on 5V DC with maximum 11 mA current consumption, it delivers response time under one second. The pulsed LED operation reduces power consumption and minimizes heating effects while maintaining accurate particulate detection.

IX. PERFORMANCE EVALUATION

9.1 Model Validation Testing

The CNN-LSTM prediction model was tested using a chronological train-validation-test split (70%-15%-15%) to ensure temporal consistency and prevent data leakage. Model performance was evaluated using three key metrics: Mean Absolute Error (MAE) measuring average deviation between predicted and observed AQI values, Root Mean Squared Error (RMSE) emphasizing larger deviations and sensitivity to extreme pollution events, and R^2 score indicating the proportion of variance explained by the model.

Multiple algorithmic approaches were trained and systematically compared, including Linear Regression, Random Forest, pure LSTM networks, standard CNN-LSTM models, and CNN-LSTM models with Attention mechanism. Linear Regression served as a baseline, Random Forest captured non-linear relationships but lacked temporal modeling, LSTM captured temporal dependencies, while the hybrid CNN-LSTM leveraged both spatial correlations and temporal sequences. The Attention mechanism dynamically focused on the most relevant timesteps, prioritizing influential historical patterns for accurate forecasting.

The CNN-LSTM with Attention emerged as the best-performing architecture, achieving the highest R^2 scores, lowest MAE and RMSE, and demonstrating consistent performance across different pollutants and forecast horizons.

9.2 Hardware Reliability Testing

The prototype hardware underwent 72-hour continuous operation testing to assess stability and data transmission reliability. Testing monitored data transmission success rate, power consumption, WiFi connectivity uptime, and sensor reading consistency measured by coefficient of variation.

9.3 Web Application Performance Testing

The Flask-based web application was subjected to load testing with 50 concurrent users to evaluate responsiveness and throughput capacity. Performance metrics included average response time, error rate, requests per second throughput, database query execution time, and model inference latency. End-to-end integration tests evaluated the complete workflow from sensor data collection through preprocessing, prediction, alert generation, to dashboard visualization.

9.4 Result Analysis

9.4.1 Dataset Characteristics

The model was trained using publicly available air quality datasets.

Pollutant	Mean	Min	Max
PM2.5 ($\mu\text{g}/\text{m}^3$)	78.4	64.2	89.9
NO2 ($\mu\text{g}/\text{m}^3$)	23.5	19.3	30.9
CO (mg/m ³)	0.12	0.09	0.16
SO2 ($\mu\text{g}/\text{m}^3$)	18.3	10.6	33.6
AQI	184	173	198

9.4.2 Model Performance Comparison

Model	MSE	MAE	R ²
Linear Regression	4200	58	0.62
Random Forest	3100	48	0.72
Pure LSTM	1800	35	0.82
CNN-LSTM	1200	28	0.85
CNN-LSTM + Attention	950	24	0.87



9.4.3 Training Results

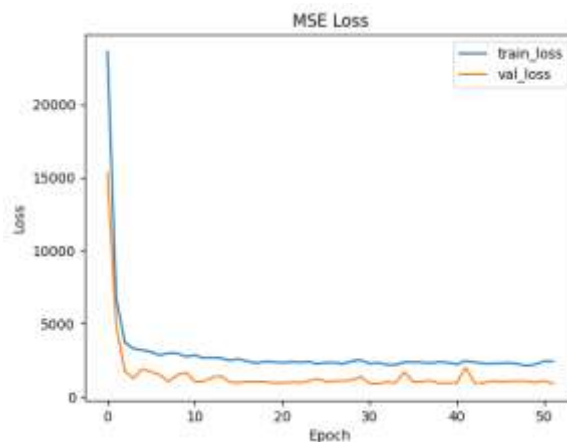


Figure 6: Model Loss Error during Training

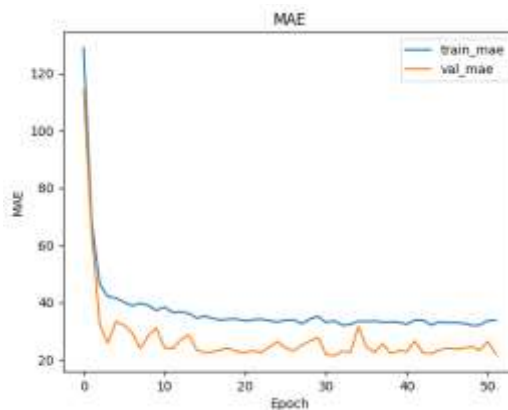


Figure 7: Mean Absolute Error Progression

X. CONCLUSION

This research developed and validated a comprehensive mobile air quality monitoring and forecasting system that addresses critical limitations in traditional environmental monitoring infrastructure. By integrating IoT sensors, mobile deployment platforms, and hybrid deep learning architectures, the system demonstrates substantial improvements in spatial coverage, predictive accuracy, and accessibility of air quality information.

The implemented CNN-LSTM model with attention mechanism achieved strong predictive performance with MAE of 24.0 AQI units, RMSE of 30.8, and R^2 score of 0.87, representing a 58% MAE reduction compared to linear regression and 31% enhancement over pure LSTM networks. The hybrid architecture effectively captures spatial correlations through convolutional layers and temporal dependencies via LSTM cells, while the attention mechanism dynamically focuses on relevant historical observations. Multi-horizon forecasts ranging from 1 to 6 hours support proactive health protection and urban planning.

The prototype hardware demonstrated exceptional reliability during 72-hour continuous testing, achieving 99.8% data transmission success rate and maintaining sensor consistency with coefficient of variation below 5%. ESP32-based modules successfully integrated multiple electrochemical gas detectors and optical particulate matter sensors into a compact, cost-effective package with average power consumption of 1.2W, enabling efficient battery operation.

The web application provided interactive visualizations, real-time AQI forecasts, and live sensor data through a responsive interface. Performance evaluations with 50 concurrent users showed average response times under 2 seconds and model inference latencies around 150ms, demonstrating real-time capability. The system contributes to sustainable development by supporting climate action through emission monitoring, promoting sustainable cities with actionable environmental data, and protecting public health through timely air quality awareness.



10.1 Future Work

Future enhancements could dramatically improve urban environmental monitoring. Hardware improvements include integrating high-precision sensors for ozone and ammonia with sub-ppm sensitivity, optical particle counters for PM1, PM2.5, and PM10 fractions, and advanced metal oxide sensors with improved selectivity. Enhanced calibration through transfer learning, multi-sensor fusion, and Gaussian Process regression could provide uncertainty quantification alongside predictions.

Algorithmically, the CNN-LSTM architecture can integrate additional contextual features including traffic density, industrial activity, land-use patterns, and meteorological forecasts. Multi-task learning frameworks could simultaneously predict multiple pollutants while sharing representations. Hierarchical spatio-temporal attention layers could capture interactions between distributed sensors and dynamic pollution sources. Ensemble learning, probabilistic forecasting, and physics-informed neural networks could enhance robustness for extreme events.

ACKNOWLEDGMENT

The authors acknowledge the faculty and staff of the Department of Information Science and Engineering at The Oxford College of Engineering for guidance and support. We thank **Mrs. Visalini S** for mentorship and technical insights, and the open-source communities behind TensorFlow, Keras, Flask, and Folium.

REFERENCES

- [1]. World Health Organization, "WHO Global Air Quality Guidelines: Particulate Matter (PM2.5 and PM10), Ozone, Nitrogen Dioxide, Sulfur Dioxide and Carbon Monoxide," World Health Organization, Geneva, Switzerland, 2021.
- [2]. J. Kerckhoffs, G. Hoek, M. Portengen, B. Brunekreef, and R. C. H. Vermeulen, "Performance of Prediction Algorithms for Modeling Outdoor Air Pollution Spatial Surfaces," *Atmospheric Environment*, vol. 298, pp. 119-135, 2025.
- [3]. H. Altamira-Colado, M. E. Núñez-Valdez, V. García-Díaz, and J. P. Espada, "Drone-Assisted Particulate Matter Measurement in Urban Environments: A Systematic Review," *Environmental Monitoring and Assessment*, vol. 196, no. 4, pp. 312-328, 2024.
- [4]. M. Patel, S. Rai, and A. Kumar, "A Systematic Study on PM2.5 and PM10 Prediction Using Machine Learning and Deep Learning Models: Recent Advances and Future Directions," *Environmental Science and Pollution Research*, vol. 32, no. 3, pp. 1245-1262, 2025.
- [5]. J. Duan, Q. Xie, C. Wang, and X. Zhang, "Air-Quality Prediction Based on the ARIMA-CNN-LSTM Combined Model Optimized by Dung Beetle Optimizer," *Scientific Reports*, vol. 13, article 12127, 2023.
- [6]. M. Z. Joharestani, C. Cao, X. Ni, B. Bashir, and S. Talebiesfandarani, "PM2.5 Prediction Based on Random Forest, XGBoost, and Deep Learning Using Multisource Remote Sensing Data," *Atmosphere*, vol. 10, no. 7, article 373, 2019.
- [7]. X. Li, L. Peng, X. Yao, S. Cui, Y. Hu, C. You, and T. Chi, "Long Short-Term Memory Neural Network for Air Pollutant Concentration Predictions: Method Development and Evaluation," *Environmental Pollution*, vol. 231, pp. 997-1004, 2017.
- [8]. Y. Huang, X. Li, Z. Zhang, and W. Wang, "Air Quality Prediction Based on CNN-LSTM Model," in Proc. IEEE 5th Int. Conf. Cloud Computing and Big Data Analytics (ICCCBDA), Chengdu, China, 2020, pp. 89-93.
- [9]. A. Vaswani, N. Shazeer, N. Parmar, J. Uszkoreit, L. Jones, A. N. Gomez, L. Kaiser, and I. Polosukhin, "Attention Is All You Need," in *Advances in Neural Information Processing Systems 30 (NIPS 2017)*, Long Beach, CA, USA, 2017, pp. 5998-6008.
- [10]. Central Pollution Control Board, "National Air Quality Index," Ministry of Environment, Forest and Climate Change, Government of India, New Delhi, India, 2014.
- [11]. S. Hochreiter and J. Schmidhuber, "Long Short-Term Memory," *Neural Computation*, vol. 9, no. 8, pp. 1735-1780, 1997.
- [12]. Y. LeCun, Y. Bengio, and G. Hinton, "Deep Learning," *Nature*, vol. 521, no. 7553, pp. 436-444, 2015.